Proceedings of the 9th U.S. National and 10th Canadian Conference on Earthquake Engineering
Compte Rendu de la 9ième Conférence Nationale Américaine et
10ième Conférence Canadienne de Génie Parasismique
July 25-29, 2010, Toronto, Ontario, Canada • Paper No 198

# DYNAMIC OCEAN WATER AND BACKFILL PORE WATER PRESSURES AGAINST A VERTICAL CAISSON DURING 2003 TOKACHI-OKI EARTHQUAKE

Isao Ishibashi[1] and Samip Pant[2]

## ABSTRACT

The heavily instrumented full scale caisson (9 m high) was constructed at the port of Kushiro, Kushiro, Hokkaido, Japan in 2001 and a major earthquake hit the site in September 2003 (M=7.5 with the maximum acceleration of 143.5 gals). The recorded date of dynamic water pressures against the caisson from the ocean side and the ones from the backfill side are analyzed and compared with the Westergaard's theoretical hydrodynamic pressure. It is found that in both cases at ocean water side and backfill side, the in-situ measured maximum dynamic water values are significantly higher than the theoretical ones. In some cases those measured values are observed as much as five times higher than the Westergaard's solution. The discrepancy is increased when the randomness on the acceleration record increased from the time segments 9-17 seconds, 17-24 seconds, and to 30-40 seconds. Since the Westergaard's theory assumes that the vibration is purely horizontal and sinusoidal, it is anticipated that the randomness of the wave forms could have generated higher dynamic water pressure in front of the caisson as well as at the backfill side of the caisson. The overlapping of incident waves and reflected waves at the wall may have caused higher water pressure response. This observed evidence during a major actual earthquake makes the current design procedure of ocean front structures more dangerous. It is suggested accordingly that commonly used Westergaard's dynamic water pressure equation shall be reexamined when it is applied on ocean front structures during earthquakes.

## Introduction

Alike the static pressures acting on retaining structures, the knowledge of dynamic pressures is equally important for safe and economical design of such structures during earthquakes. The additional dynamic pressures exerted due to the ocean water and backfill soil, if not considered seriously, could be the cause of failure of waterfront structures.

The dynamic earth pressure against rigid retaining structures is commonly calculated by Mononobe-Okabe's method (Mononobe 1924, Okabe 1924). For water front structures, in addition, dynamic water pressures shall be added to the dynamic earth pressure. Ishibashi et al. (1994) proposed a comprehensive procedure to handle dynamic earth pressure as well as dynamic water pressure against rigid retaining walls during earthquakes with saturated backfill

[1]Professor, Dept. of Civil and Env. Engineering, Old Dominion University, Norfolk, VA 23529
[2]Former graduate student, Dept. of Civil and Env. Engineering, Old Dominion University, Norfolk, VA 23529

soils. In the theory, dynamic water pressure on the backfill side is nearly equal to the one by Westergaard's solution (Westergaad 1933) for highly porous backfill materials like gravels and coarse sands. On the other hand, for the backfills of low permeable soils like clayey soils, dynamic pore water pressure is mainly due to soil's compressibility. On the water side of the walls, dynamic water pressure against the walls will be considered to have the full value of Westergaard's solution. Ishibashi et al.'s hypothesis is made based on their shaking table model study, which used sinusoidal wave forms and thus it has not been tested under actual random earthquake vibration signals.

In 2001 in Japan, a full scale caisson quaywall was constructed at Port of Kushiro (Sasajima et al. 2003). The port is located at a highly active seismic region and large earthquakes are anticipated there in near future. The quaywall was heavily instrumented with accelerometers, velocimeters, earth pressure cells, pore water pressure cells, and inclinometers and it was ready to receive major earthquakes. Several major earthquakes hit the site and the obtained data were analyzed. For example, an analysis for liquefaction was reported by Sasajima et al. (2005). This paper analyzes the data obtained for pore water pressure at both water side and backfill side in order to reveal dynamic pore water pressure generation due to random earthquake signals. The data is compared fully with Westergaard pressure for the water side of the wall and with Ishibashi et al.'s hypothesis for the backfill side of the wall.

## Port of Kushiro and Earthquakes

The observation site for the dynamic behavior of the quaywall was located in the Port of Kushiro, Eastern Hokkaido, Japan. The construction and installation of the observation system were accomplished by March 2001. The observation was started in April 2001 and was scheduled to terminate at the end of March 2005. During the observation period the strongest earthquake recorded at the site was Kushiro-Oki earthquake on Sep 26, 2003 which was of magnitude 7.8 (Richter Scale) and Intensity 5 (Modified Mercalli) at the Kushiro Port. This record was used for the analysis in this paper

## Quaywall Construction with Instrumentation

Three caissons were placed in a row in the East-West direction and two outside test caissons were used for instrumentation. The caissons were designed to have a safety factor against sliding of 1.0 for earthquake motion whose horizontal acceleration is 100 gals, on the basis of the current standard design procedure. The test caissons were cast on the ground, and then earth pressure cells, accelerometers, and velocimeters were mounted in dry condition. The seabed was excavated and a rubble mound was prepared with coarse gravel. The caissons were then placed on top of the rubble mound. The backfill ground was then reclaimed with dredged fine sand. The reclaimed backfill ground was separated into two sections by a row of sheet piles. The east section was treated against liquefaction with sand compaction pile method and the west section was not treated at all. Before the treatment, N-value from standard penetration test (SPT) of the reclaimed backfill was 4. However, it was increased to 20 in the treated region. In this analysis the records only at the treated site are used since the objective of this research is to find dynamic water pressure generation due to earthquake vibration, not the effect of liquefaction. The cross-sectional profile of this caisson with instrumentation is shown in Fig.1.

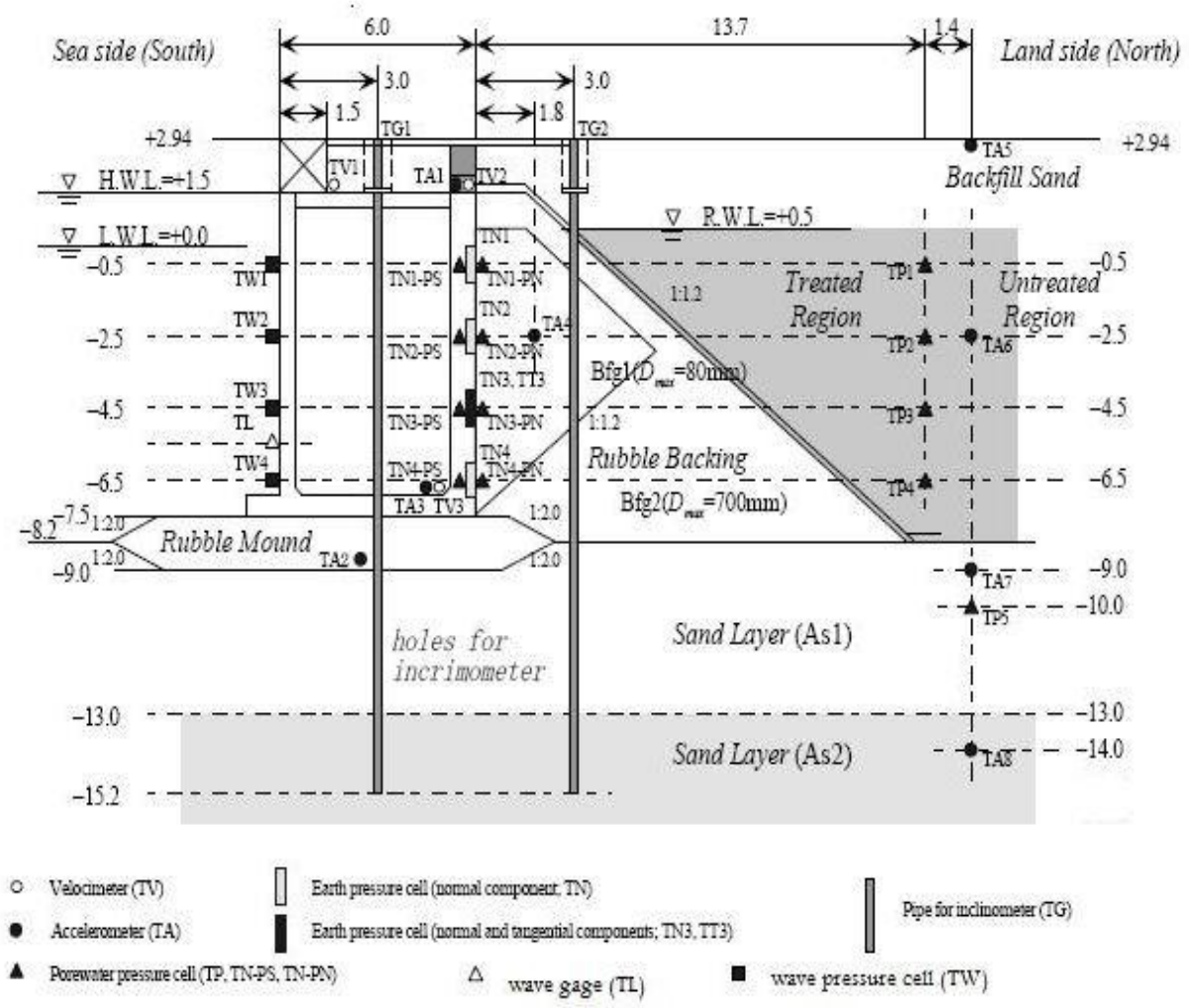


Fig.1 Cross-section of caisson quaywall (treated backfill) with instrumentations

For this caisson, eight three-components (X, Y and Z) accelerometers (TA1-8) three three-components velocimeters (TV1-3) were installed as seen. On the front wall (water side) of the test caisson four water pressure cells (TW 1-4) were vertically arranged to measure the change in dynamic water pressure induced by the ocean water. Also a wave gage TL was installed on the front wall of the caisson to monitor the wave height fluctuation. On the back of the test caisson pore water pressure cells (TP1-5) were arranged in vertical arrays to measure the dynamic pore water pressure during earthquakes. Four earth pressure cells were also vertically arranged (TN1-4). An inclinometer was installed in order to monitor the displacement of the test caissons and backfill ground induced by large earthquakes. The electric signals from all sensors were converted from analogue to digital and collected in a main computer set at the observatory house setup beside the test quaywall. The system was designed to start automatically measurements when the accelerometer TA8 at the base layer (El –14 m) got the threshold value.

## Recorded Data and Analysis

### Recorded data

The September 26, 2003 Kushiro-oki earthquake was the strongest earthquake recorded during the observation period of the project. It had magnitude 7.8 and an intensity 5 at Kushiro Port. The maximum acceleration exceeded a hundred gals at the top of the test caissons and the horizontal displacements of the test caissons about 20 cm were recorded after the earthquake. The untreated region had observed soil liquefaction. Only data from the treated area is analyzed, since the objective of this project is to verify the Westergaard's hydrodynamic theory with measured dynamic ocean water on the ocean side and dynamic pore water pressure on the backfill due to a random earthquake vibration. The earth pressure data was not taken into account for this study.

Westergaard's theory assumes that vibrations in the earthquake are horizontal in a direction perpendicular to the vertical face of the dam. The North-South direction is the one that is perpendicular to the vertical wall of the caisson and this is represented by X-direction in the record. For example TA1X represents the accelerometer 1 at the treated region measuring vibration in North-South direction. The plot for TA2X is shown in Fig. 2 and typical records of pore water pressure at backfill side (at TN1PN), water pressure at ocean side (TW1), and wave gauge at TL are shown in Fig. 3, 4 and 5, respectively.

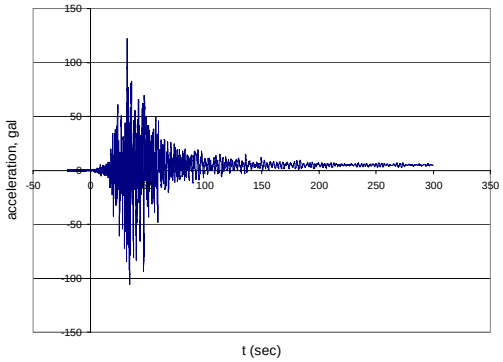


Fig.2 Acceleration vs. time at TA2X

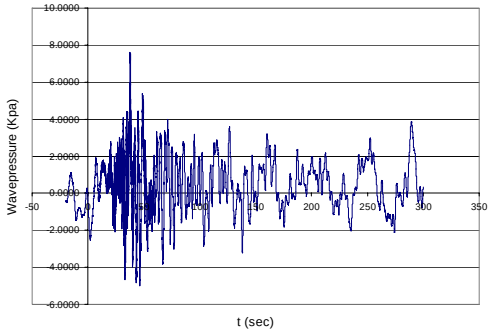


Fig.4 Ocean water pressure (uncorrected) vs. time at TW1

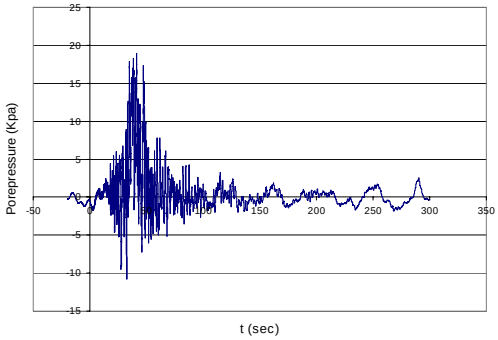


Fig.3 Pore water pressure vs. time at TN1PN

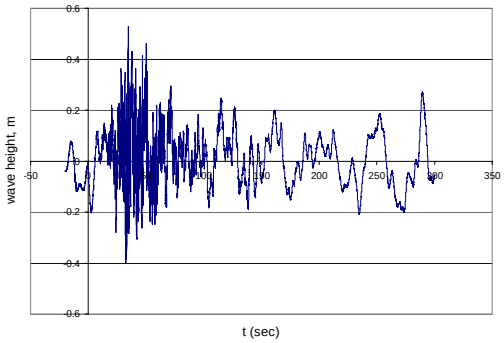


Fig.5 Wave height vs. time at TL

Table 1. Maximum values of the records and corresponding times

| Sensor | Max Value, gal | Time, sec | Sensor | Max Value, kPa | Time, sec |
|---|---|---|---|---|---|
| TA1X | 136.724 | 32.31 | TN1PN | 18.909 | 41.19 |
| TA2X | 122.424 | 32.25 | TN2PN | 20.448 | 41.19 |
| TA3X | 145.392 | 32.02 | TN3PN | 21.058 | 41.18 |
| TA4X | 102.833 | 34.38 | TN4PN | 20.43 | 41.8 |
| TA5X | 156.974 | 32.2 | TW1 | 7.597 | 37.76 |
| TA6X | 135.28 | 32.16 | TW2 | 8.39 | 37.76 |
| TA7X | 165.264 | 35.98 | TW3 | 9.333 | 37.76 |
| TA8X | 125.608 | 35.95 | TW4 | 10.101 | 37.76 |
| | | | Sensor | Max Value, m | Time, sec |
| | | | TL | 0.528 | 34.37 |

The maximum values of those records and their corresponding times are summarized in Table 1. From the above tables, it is observed that the maximum acceleration (TA) occurs between the time interval 32 to 36 seconds. Maximum values of pore pressure (TN) from backfill soil are observed later than peak acceleration, i.e., 41 to 42 seconds. Ocean water pressure (TW) peaks are observed slightly later than the peak acceleration at time 37.76 second, and the maximum wave height (TL) recorded by the wave gage occurred at nearly the same time as the peak acceleration.

**Fourier spectra of earthquake signal**

In order to see the effect of wave form on measured water pressures, the measured acceleration record TA2X (Fig.2) was divided into three time segments. First one is at very early stage, 9 to 17 seconds when only minor vibration is recorded. Second segment was between 17 to 24 seconds when the average vibration is recorded, and the third one was at the segment between 30 to 40 seconds when the maximum vibration is observed. The vibration subsides gradually after 50 seconds. Frequency analyses by Fast Fourier transform were conducted in Figs. 6 (a), (b) and (c) for each segment of the acceleration record, respectively.

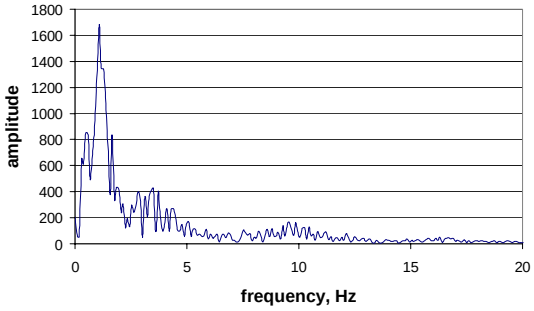


(a) t= 9 and 17 sec

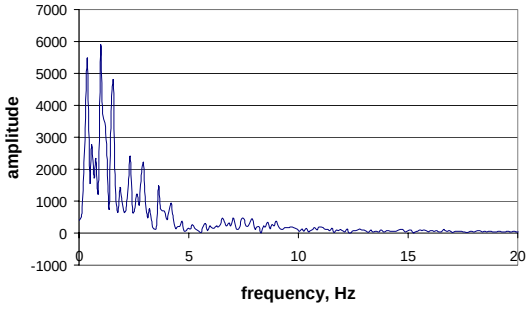


(b) t= 17 and 24 sec

Fig.6 (a) and (b) Fourier spectra of acceleration record at TA2X

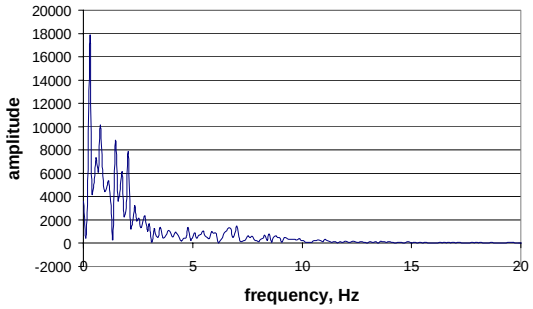


Fig.6 (c) Fourier spectra of acceleration record at TA2X (t=30 and 40 sec)

From those Fourier spectra, at the earlier stage of the vibration (t=9-17 sec.) a rather simple vibration mode with predominant frequency with 1.0 Hz is observed (Fig.6(a)). At the mid-stage (t=17-24 sec.), three dominant frequencies appeared (Fig.6(b)). At the later stage (t=30-40 sec.), one dominant frequency with 0.3 Hz and three other dominant frequencies are observed (fig.6(c)). Those observations indicate that the transmitted wave form increases its randomness with increasing time. These figures depict the fact that earthquake signals are summations of direct arrivals of the various waves and their refracted and reflected waves.

**Ocean side dynamic water pressure**

Ocean side water is free from any backfill soils and thus the results are fully compared with Westergaard's solution. The recorded data at four water pressure cells TW1, TW2, TW3, and TW4 at the ocean side of the wall were analyzed. In order to obtain purely dynamic water pressure against the wall due to earthquake vibration, the effect of ocean wave action on water pressure was corrected. This is done with the utilization of the data recorded by the wave gage TL (Fig.5). The pressure given by the height of water on TL measurement was subtracted from the water pressure recorded by water pressure cells for the analysis.

Acceleration record atTA2 was chosen as the reference acceleration data to analyze ocean water pressure records because it was located at the rubble mound that is just below the caisson and nearest to the wave pressure sensors. Local peak water pressures on the records were searched after local peak accelerations were identified for the entire vibration time domain. Fig.7 (a), (b), and (c) show some comparisons of the measured peak pressure distributions with Westergaard's theoretical solutions at different time segments of the vibration.

Westergaard's solution for dynamic water pressure $p_{wd}$ is given by;

$$p_{wd} = \frac{7}{8} x\, \gamma_w \; x\, k_h \times \sqrt{H_w x\, X} \qquad (1)$$

Where $k_h$ is the horizontal coefficient of earthquake vibration ($=a_h/g$) .The local peak acceleration $a_h$ at TA2X record, which preceded the local peak water pressure, is used. $H_w$ is the total depth of water and X is the depth of the wave pressure gages. Since the exact location of the datum adopted by the TL (wave gage) is not known, the datum was assumed in between the low water level and the high water level and thus Westergaard's pressures are calculated from both low water level and high water level in the figures.

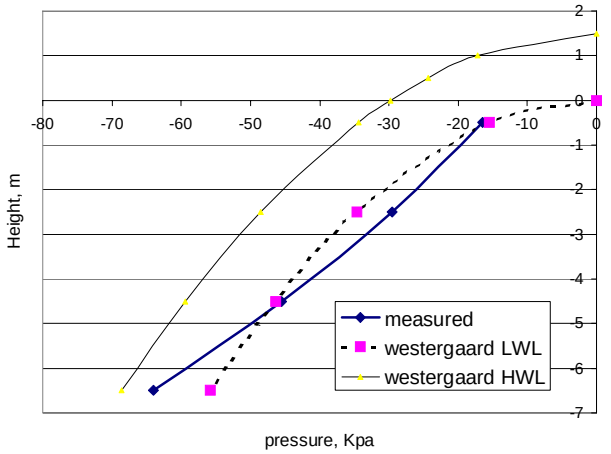


(a) at t = 16.81 sec (for 9-17 sec segment)

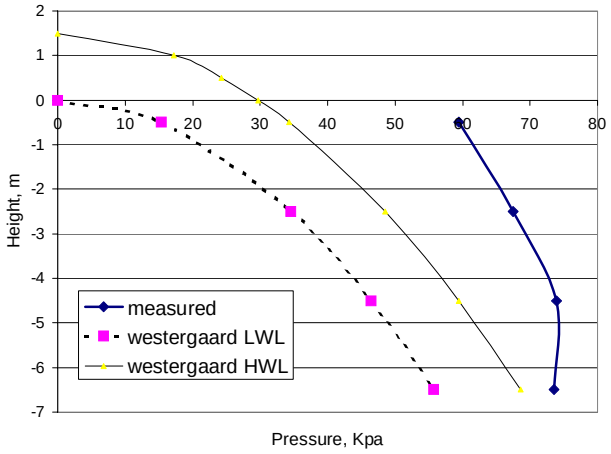


(b) at t = 19.18 sec (for 17-24 sec segment)

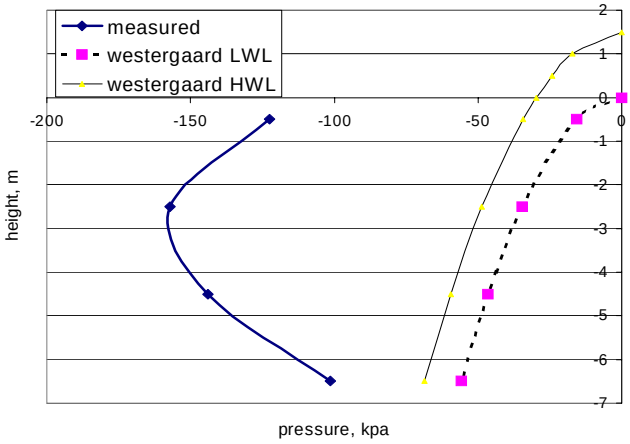


(c) at t=30.27 sec (for 30-40 sec segment)

Fig.7 Comparison of dynamic water pressures at ocean side of wall

It is observed from Fig.7 that the measured water pressures and Westergaard's value are in good agreement for t=9-17 second segment data. For t=17-24 second and t= 30-40 second data, the measured values are higher than the Westergaard's pressure. The discrepancy between those increased with time increased. The distribution curves seem to follow approximately parabolic shape proposed by Westergaard's theory.

**Backfill side dynamic water pressure**

As seen in Fig.1, rubble backfill is placed just behind the wall. According to Ishibashi et al. (1994), in gravel backfill, pore water in backfill is nearly free to move in void due to application of inertia force and thus the wall will subject to nearly 100 % of Weastergaad's solution. And gravel is less compressive so that dynamic water pressure due to soil's compressibility will be negligible. On that hypothesis, anticipated dynamic water pressure at the backfill side can be compared with the Westergaard's solution. Fig.7 (a), (b), and (c) show the comparisons between hydrodynamic pressure in backfill soil and Westergaard's pressure for those different time segments.

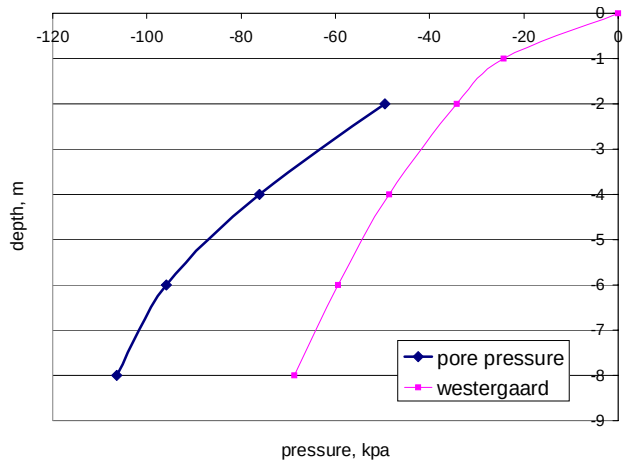


(a) at t = 9.54 sec (for 9-17 sec segment)

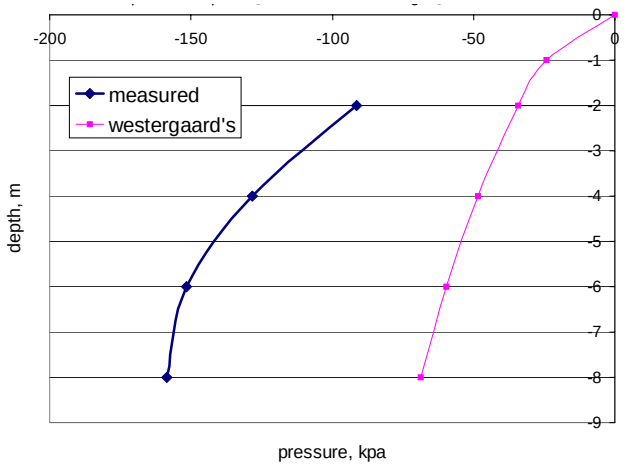


(b) at t = 17.08 sec (for 17-24 sec segment)

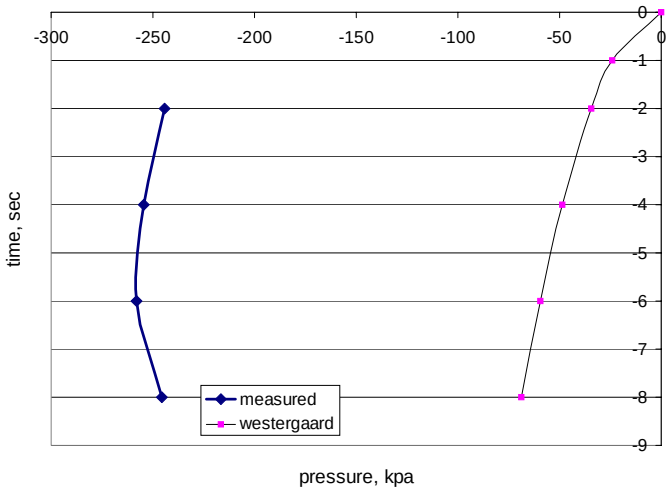


(c) at t = 33.5 sec (for 30-40 sec segment)

Fig.7 Comparison of dynamic water pressures at backfill side

Like in the ocean side pressures, measured backfill side dynamic water pressures are also rather close to Westergaard's for earlier stage of the earthquake and it is much larger than the Westergaar's at the later stage.

**Discussion of the results**

In both cases (ocean side and backfill side), measured dynamic water pressures were rather close value to Westergaard's solution at the earlier stage of vibration. At the later stage of vibration, measured ones were much larger than the Westergaard's. Westergaard theory assumes sinusoidal horizontal vibration and Ishibashi et al.'s shaking table model study also used sinusoidal wave. The recoded data used for this study were, however, due to a random earthquake signal. Fourier spectra of acceleration record in Fig.2 showed that it had rather a single dominant frequency in the earlier stage of vibration, where the recorded data and the theory were in closer agreement. At later stage, several dominant frequency components were

observed and the randomness of signal is increased and so does the discrepancy of the results. Considering the fact that the randomness of wave form will come from overlaps, refraction, and reflection of waves, the dynamic water pressure will also be influenced by the randomness of wave signals. Dynamic water pressure is indeed due to horizontal compressive wave propagation through the body of water and thus induced pressure will be enlarged or reduced depending on arrival timings of those random wave signals.

## Conclusions

The heavily instrumented full scale caisson (9 m high) at Kushiro Port was subjected to a major earthquake and the measured dynamic water pressures at ocean side as wells as at backfill side were analyzed in comparison with Westergaard's for the ocean side and with Ishibashi et al.'s for backfill side of the wall. It was found that in both sides the measured maximum dynamic water values are higher than the theoretical ones. It was found that the discrepancy increased from the earlier stage to the later stage of the vibration, where the randomness of the earthquake signal also increased in the acceleration record. The overlap of incident waves and reflected waves at the wall due to random vibration signal may have caused higher dynamic water pressure response. This observed evidence during a major actual earthquake makes the current design procedure of ocean front structures more dangerous and Westergaard's dynamic water pressure theory shall be reexamined when it will be applied to ocean front structures during random earthquake vibration signals.

## Acknowledgement

The authors acknowledge Civil Engineering Research Institute of Hokkaido for publically opening the valuable data and also acknowledge Drs. Takahiro Sugano and Tomohiro Tanaka of Port and Airport Research Institute for their assistance in obtaining detailed data.

## References

Ishibashi, I., Osada, M., Uwabe, T.,1994. Dynamic Lateral Pressures Due to Saturated Backfills on Rigid Walls, *Journal of Geotechnical Engineering*, Vol. 120, No.10, pp. 1747-1767.

Mononobe, N., 1924. Considerations into Earthquake Vibrations and Vibration Theories, *Journal of Japan Society of Civil Engineers*, Vol. 10, No. 5, pp. 1063-1094.

Okabe, S.,1924. General Theory on Earth Pressure and Seismic Stability of Retaining Wall and Dam, *Journal of the Japan Society of Civil Engineers*, Vol. 10, No. 5, pp. 1277-1323.

Sasajima, T., Sakikawa, M., Miura, K., Otsuka, N., 2003. In-situ Observation System for Seismic Behavior of Gravity Type Quay Wall, *Proceedings of Thirteenth International Offshore and Polar Engineering Conference*, Hawaii, USA, pp.742-749.

Sasajima, T., Miura, K., Kubouchi, A., Otsuka, N., Kohama, E., and Watanabe, J., 2005. Liquefaction Induced Deformation of Test Quay Wall in Kushiro Port during the 2003 Tokachi-oki Earthquake, *Proceedings of the Geo-Frontiers 2005*, Austin, Texas, USA.

Westergaard, H.M.,1933. Water Pressures on Dams During Earthquakes, *Transactions of the American Society of Civil Engineers*, Vol. 98, pp. 418-433.